LIMNOLOGY and OCEANOGRAPHY

ASLO

Limnol. Oceanogr. 9999, 2023, 1–16

doi: 10.1002/lno.12381

P inputs determine denitrifier abundance explaining dissolved nitrous oxide in reservoirs

Elizabeth León-Palmero [1*,a], **Rafael Morales-Baquero** [1], **Isabel Reche** [1,2*]

[1]Instituto del Agua and Departamento de Ecología, Universidad de Granada, Granada, Spain
[2]Research Unit Modeling Nature (MNat), Universidad de Granada, Granada, Spain

Abstract

Reservoirs are important sites for nitrogen processing, especially those located in agricultural and urban watersheds. Nitrogen inputs promote N_2O production and emission, but the microbial pathways controlling N_2O have been seldom studied in reservoir water columns. We determined N_2O concentration in the water column of 12 reservoirs during the summer stratification and winter mixing. We explored the potential microbial sources and sinks of N_2O by quantifying key genes involved in ammonia oxidation (bacterial and archaeal *amoA*) and denitrification (*nirS* and *nosZ*). Dissolved N_2O varied up to three orders of magnitude (4.7–2441.2 nmol L^{-1}) across systems, from undersaturated to supersaturated values (37%–24,174%) depending on reservoirs and depths. N_2O concentration depended on nitrogen and oxygen availabilities, with the lowest and highest N_2O values at suboxic conditions. Ammonia-oxidizing archaea dominated over ammonia-oxidizing bacteria but were not related to the dissolved N_2O. In contrast, the abundance of the *nirS* gene was significantly related to N_2O concentration, and three orders of magnitude higher than *amoA* abundance. Denitrifying bacteria appeared consistently in the water column of all reservoirs. The *nirS* and *nosZ* genes appeared in oxic and suboxic waters, but they were more abundant in suboxic waters. The nitrate concentration, and *nirS* and *nosZ* relative abundances explained the dissolved N_2O. Besides, *nirS* abundance was related positively with total phosphorus and cumulative chlorophyll *a*, a proxy for fresh organic matter. Therefore, P inputs, not just N inputs, promoted N_2O production by denitrification in the water column of reservoirs.

The anthropogenic production of fertilizer has doubled the inputs of nitrogen (N) to the Earth's surface, increasing their exports to freshwaters and boosting the production of nitrous oxide (N_2O) (e.g., Seitzinger et al. 2000; Beaulieu et al. 2011). N_2O is a potent greenhouse gas with 298 times the warming effect of CO_2 in a 100-yr time horizon (IPCC 2013) and the primary driver of stratospheric ozone depletion (Ravishankara et al. 2009). The studies on N_2O emissions in freshwaters have mainly focused on streams and rivers (Beaulieu et al. 2015), with an estimated N_2O emission of 0.68 Tg N_2O-N yr^{-1} (Beaulieu et al. 2011). Nevertheless, the longer water residence time of lentic systems such as lakes and reservoirs results in substantial N processing (Wetzel 2001). The N_2O emission from lakes and reservoirs was recently estimated at ~ 0.3 Tg N_2O-N yr^{-1} based on a scarce dataset (DelSontro et al. 2018). Reservoirs are enlarged water bodies behind a dam, and their number has increased significantly over the past 60 years, reaching over 16.7 million globally (Lehner et al. 2011). In spite of this, reservoirs are particularly understudied, although they process a disproportionately high fraction of N from the catchment in comparison to lakes due to their higher catchment area, and higher drainage ratio (i.e., the catchment area: lake or reservoir surface area) (Harrison et al. 2009). They may support exceptionally high N_2O emissions due to substantial N loadings from the agricultural and urban areas in their watersheds, exceeding punctually the climatic forcing produced by CH_4 emissions (e.g., Iznájar reservoir

*Correspondence: eleonpalmero@ugr.es; ireche@ugr.es

Additional Supporting Information may be found in the online version of this article.

[a]Present address: Nordcee, Department of Biology, University of Southern Denmark, Odense, Denmark

Author Contribution Statement: E.L.-P., R.M.-B., and I.R. contributed to data acquisition during the reservoir samplings. E.L.-P. analyzed the samples and processed the data. E.L.-P., R.M.-B., and I.R. analyzed the data and discussed the results. E.L.-P. wrote the first draft manuscript, which was complemented by significant contributions of R.M.-B. and I.R. I.R. and R.M.B. designed the study and obtained the funds. All authors have given approval to the final version of the manuscript.

in León-Palmero et al. 2020*a*). Therefore, a better understanding of the controlling factors that lead to N_2O production and consumption in the water column of reservoirs is needed, especially regarding the increasing trend in reservoir construction at a global scale (Zarfl et al. 2015).

Microbial nitrification and denitrification produce N_2O. Nitrification consists of the oxidation of ammonia to nitrite (i.e., ammonia oxidation) and to nitrate (i.e., nitrite oxidation). Ammonia oxidation is the rate-limiting step, and it is performed by ammonia-oxidizing bacteria (AOB) and ammonia-oxidizing archaea (AOA) (Kowalchuk and Stephen 2001; Könneke et al. 2005). The global significance of this process and the relative contribution of AOB and AOA have been deduced from the abundance of the bacterial and the archaeal *amoA* genes, which encode the subunit A of the key enzyme ammonia monooxygenase (Kowalchuk and Stephen 2001; Francis et al. 2005). N_2O is a by-product of AOB and AOA in oxic conditions through different pathways (Ward 2013*a*; Stein 2019). While N_2O production in AOB occurs through enzymatic activity via the two obligate intermediates hydroxylamine (NH_2OH) and nitric oxide (NO) (Caranto and Lancaster 2017); the N_2O formation in AOA seems to be a hybrid process, where NO reacts with NH_2OH (Kozlowski et al. 2016), although specific details persist controversial. At low oxygen conditions, AOB also performs nitrifier denitrification, which consists of reducing nitrite to NO and N_2O, increasing the yield of N_2O produced relative to the ammonia oxidized (Wrage et al. 2001; Ward 2013*a*). For both cases, N_2O production rates reached maxima at suboxic conditions ($< 10\ \mu mol\ L^{-1}$) (Hink et al. 2017). AOA are present in marine waters and sediments in large numbers, contributing significantly to the N_2O production (e.g., Francis et al. 2005; Löscher et al. 2012). However, the contribution of ammonia-oxidizing microorganisms to dissolved N_2O in reservoirs has not been studied.

Denitrification consists of the subsequent reduction of nitrate to nitrite, NO, N_2O, and dinitrogen (N_2), generally coupled to the oxidation of organic matter. It can be a source or a sink of N_2O depending on the rate of N_2O production compared to the rate of N_2O reduction to N_2. The genes that code the nitrite reductases (i.e., *nirS, nirK*) during denitrification are widely used to infer the abundance and the contribution of the denitrifying bacteria to the dissolved N_2O budget, while the gene that code the nitrous oxide reductase (i.e., *nosZ*) is used to address the capacity of reducing N_2O to N_2 (Hallin et al. 2018). Besides, denitrification is usually considered as a facultative anaerobic respiration because oxygen regulates the sequence of the denitrification enzymes, especially the nitrous oxide reductase coded by *nosZ*, which is inhibited even at very low oxygen concentrations (Bonin et al. 1989; Dalsgaard et al. 2014). Consequently, the studies on denitrification in freshwaters have focused on anoxic waters, particularly, on sediments (Piña-Ochoa and Álvarez-Cobelas 2006). However, denitrifiers are also present in the water column of lakes (Junier et al. 2008; Kim et al. 2011; Pajares et al. 2017), and the influence of O_2 concentration on the denitrifying activity appears to differ from one bacterium to another (Lloyd 1993).

Lakes and reservoirs can be essential players in the N removal at the landscape scale, acting as N_2O sources in areas subjected to high N inputs (McCrackin and Elser 2011) or N_2O sinks as, for instance, in boreal lakes (Soued et al. 2015). However, only some studies have focused on the role of reservoirs as sinks or sources of N_2O, specially regarding their water columns. Here, we quantified the dissolved N_2O concentration during the summer stratification and the winter mixing in the water column of 12 temperate Mediterranean reservoirs covering a broad spectrum of ages, morphometries, chemical characteristics, and watershed land uses. We examined the main drivers of N_2O concentration in the water column. We also studied the relationship between the nitrifiers and denitrifiers abundance and the N_2O concentration. Finally, we connected the landscape and the chemical and biological properties to provide an ecosystemic perspective of N_2O cycling in reservoirs.

Material and methods

Study reservoirs, morphometry, and watershed land uses

We sampled the water column of 12 reservoirs located in southern Spain between July 2016 and August 2017, once during summer stratification and once during winter mixing. The location of these reservoirs is shown in Supporting Information Fig. S1a,b. The study reservoirs were built between 1932 and 2003 for water supply and agriculture irrigation, and they differ in morphometry, water chemistry, and trophic status. In Supplementary Table S1, we showed the geographical coordinates, age, and the morphometric description of the study reservoirs. They are in watersheds with contrasting land uses, ranging from forested landscape (e.g., San Clemente reservoir in Supporting Information Fig. S1c) to agricultural and urban landscape (e.g., Iznájar reservoir, in Supporting Information Fig. S1d). We provided more information and detailed maps in León-Palmero et al. (2019, 2020*a*,*b*,*c*,*d*).

Water column sampling

Vertical profiles and water column sampling were performed near the dam, in the open waters of the reservoir, selecting the same location during the stratification and the mixing period. First, we performed the vertical profile using a Sea-Bird 19plus CTD profiler. Then, based on the temperature and oxygen profiles, we selected six to nine depths representing the epilimnion, metalimnion (oxycline), and hypolimnion. We took the water samples at these depths using a 5-l UWITEC sampling bottle for the chemical and biological analysis explained below. We selected 178 depths in total, 96 depths during stratification and 82 depths during mixing. From these samples, the concentrations of the dissolved N_2O

and chlorophyll *a* (Chl *a*), and the abundance of prokaryotes were analyzed. For the analysis of the major nutrients and functional genes, we selected three or four representative depths of the epilimnion, metalimnion (oxycline), and hypolimnion, or bottom waters during the stratification period ($n = 41$), and three or four equivalent depths during the mixing period ($n = 36$).

Dissolved N_2O in the water column

Samples for the dissolved N_2O analysis were carefully collected in 125 or 250 mL airtight Winkler bottles in duplicate (250 mL) or in triplicate (125 mL), preserved with a solution of $HgCl_2$ (final concentration 1 mmol L^{-1}) to inhibit biological activity, and sealed with Apiezon® grease to prevent gas exchange. We stored these samples in the dark at controlled temperature (25°C) until analysis. We measured dissolved N_2O using headspace equilibration in a 50 mL airtight glass syringe (Agilent P/N 5190–1547; Sierra et al. 2017). We obtained two replicates for each 125 mL Winkler bottle and three replicates for each 250 mL Winkler bottle. We took a quantity of 25 g of water (± 0.01 g) using the airtight syringe and added a quantity of 25 mL of a standard gas mixture that had a N_2O concentration similar to atmospheric values (0.3 ppmv) to complete the volume of the syringe. The syringes were shaken for 5 min (Vibromatic, Selecta) to ensure mixing, and we waited 5 min to reach complete equilibrium. Then, the gas in the syringe was injected manually into the gas chromatograph (GC; Bruker® GC-450). We daily calibrated the detectors using three standard gas mixtures with N_2O concentrations of 305, 474, 2000 ppbv, made and certified by Air Liquide (France). The precision for the gas mixture of N_2O used in the headspace equilibrium (0.3 ppmv) was 7.8% ($n = 108$). We calculated the gas concentration in equilibrium using the Bunsen solubilities for N_2O (Weiss and Price 1980). The precision of the measurement of the dissolved N_2O concentration, that included the analytical processing of the samples and the equilibration step, was 3.1% (N_2O) for four to six replicates of each sample. We calculated the saturation values (%) as the ratio between the concentration of the dissolved gas measured and the gas concentration expected in equilibrium considering the temperature, salinity, and barometric pressure of each reservoir.

Chl *a* and major nutrient analysis in the water column

Water samples for chemical and biological analysis were maintained at 4°C until arrival at the laboratory. We determined Chl *a* concentration by filtering the particulate material of 500 to 2000 mL of water through 0.7 μm pore-size Whatman GF/F glass-fiber filters. Then, we extracted the pigments from the filters with 95% methanol in the dark at 4°C for 24 h (APHA 1992). We measured Chl *a* absorption at the wavelength of 665 nm using a Perkin Elmer UV-Lambda 40 spectrophotometer, and we corrected the solution scattering at 750 nm. To obtain the cumulative Chl *a* in the whole water column (mg Chl *a* m^{-2}), from the discrete depths, we added the concentration of Chl *a* from each stratum using the trapezoidal rule as described previously (León-Palmero et al. 2020*b*).

We used the filtered water to determine the concentrations of dissolved nutrients, and the unfiltered water for total nutrients. We acidified the samples for dissolved organic carbon (DOC), total dissolved nitrogen (TDN), and total nitrogen (TN) concentration with phosphoric acid (final pH < 2). We measured DOC, TN, and TDN by high–temperature catalytic oxidation using a Shimadzu total organic carbon analyzer (Model TOC-V CSH) coupled to nitrogen analyzer (TNM-1; Álvarez-Salgado and Miller 1998). We measured the nitrate (NO_3^-) concentration using the ultraviolet spectrophotometric method with a Perkin Elmer UV-Lambda 40 spectrophotometer at the wavelength of 220 nm and including corrections for DOC absorbance at 275 nm (APHA 1992). We measured the nitrite (NO_2^-) concentration by inductively coupled plasma optical emission spectrometry. In this work, we calculated the dissolved inorganic nitrogen as the addition of the NO_3^- and NO_2^- concentrations. We measured total phosphorus (TP) concentration by triplicate using the molybdenum blue method after digestion with a mixture of potassium persulfate and boric acid at 120°C for 30 min (APHA 1992).

Abundance of prokaryotes

The abundances of total prokaryotes were determined using flow cytometry in unfiltered water following the procedures proposed by Gasol and del Giorgio (2000). We collected and fixed the samples with a mixture of 1% paraformaldehyde and 0.05% glutaraldehyde for 30 min in the dark at 4°C. Then, we froze the samples in liquid nitrogen and stored them at −80°C until analysis. We analyzed the samples in triplicate in a FACScalibur flow cytometer equipped with the BD CellQuest Pro software for data analysis. Before analysis, we stained the samples (500 μL) for 10 min in the dark with a DMSO diluted SYBR Green I (Molecular Probes) stock (1 : 200) at 10 μmol L^{-1} final concentration. We used yellow–green 0.92 μm latex beads (Polysciences) as an internal standard to control the cytometer performance every day. Samples were run at low speed for 2 min and detected by their signature in bivariate plots SSD vs. FL1 (green fluorescence of the DNA stained with SYBR Green I).

Quantitative PCR (qPCR) assays

We quantified the abundance of unique functional genes involved in N_2O cycling using qPCR. We also calculated the ratio between the abundances of the specific genes (copies mL^{-1}) and total prokaryotes (cell mL^{-1}) to distinguish the effect of different chemical and biological drivers on the total abundance of prokaryotes vs. the abundance of the specific groups. We targeted the *amoA* gene, which encodes the catalytic subunit of ammonia monooxygenase (Kowalchuk and

Stephen 2001), to study the AOB (bac-*amoA*), and the AOA (arch-*amoA*). To study the denitrifier abundance, we targeted the *nirS* and the *nosZ* genes. The *nirS* gene encodes the nitrite reductase that catalyzes the transformation of nitrite to NO, while the *nosZ* gene encodes the nitrous oxide reductase, that reduces N_2O to N_2. We chose specific primers from previous studies performed in freshwaters. Pure cultures were used as positive controls in PCR, and for qPCR standard preparation. Primers, amplicon length, annealing temperature, and pure cultures are shown in Supplementary Table S2. We provide further details on the DNA extraction and qPCR procedure in the Supporting Information (Extended Materials and methods).

Statistical tests and software

We used linear regression analysis and generalized additive models (GAMs) (Wood 2006). We examined the concurvity among predictors and fitted the models to minimize the Akaike information criterion and the generalized cross validation criterion values. We conducted all the statistical analysis in R software (R Core Team 2019). We also used R and Inkscape™ (Inkscape Project 2017) to plot the results and create the figures. We provide further details on the statistical analysis performed in the Supporting Information (extended materials and methods).

Results and discussion

Profile description: N_2O sinks vs. sources

We found prominent changes in the dissolved N_2O concentration among reservoirs, depths, and seasons (Figs. 1, 2, Supporting Information Figs. S2–S11 and summarized in Supplementary Table S3). The N_2O concentration and % of saturation ranged up to three orders of magnitude from 4.7 to 2441.2 nmol L^{-1}, and from 37% to 24,174%. To facilitate the result presentation, we grouped the reservoirs as sinks if the sum of the N_2O fluxes during the summer stratification and winter mixing was ≤ 0; or sources if the sum was > 0 according to our previous study on N_2O fluxes in these 12 reservoirs (León-Palmero et al. 2020*a*). The eight reservoirs that acted as N_2O sinks (hereafter, sinks) were: San Clemente, La Bolera, Francisco Abellán, Jándula, Negratín, El Portillo, Rules, and Los Bermejales (Fig. 1; Supporting Information Figs. S2–S8). The four reservoirs that acted as sources of N_2O (hereafter, sources) were: Iznájar, Béznar, Cubillas, and Colomera (Fig. 2; Supporting Information Figs. S9–S11). N_2O concentration in the water column of the sinks varied from 4.7 to 46.1 nmol L^{-1} (median = 12.3 nmol L^{-1}), and from 12.6 to 2441.2 nmol L^{-1} in the sources (median = 20.3 nmol L^{-1}). While the sources were always supersaturated in N_2O (109%–24,174%), the sinks showed supersaturation and undersaturation at different depths of the same profile (37%–366%). The median concentration and % of N_2O in the sinks were lower than in the sources (Supporting Information Fig. S12). We detected the minimum value of N_2O in the hypolimnion of San Clemente (4.7 nmol L^{-1}, 37%, Fig. 1a), and the maximum value in the hypolimnion of Iznájar (2441.2 nmol L^{-1}, 24,174%, Fig. 2a); both of them at suboxic conditions (i.e., DO < 10 μmol L^{-1}). These two reservoirs also showed the minimum and maximum N_2O fluxes in León-Palmero et al. (2020*a*). In addition, we also observed N_2O undersaturation at other depths of the water column in oxic conditions, as in La Bolera, Negratín, and El Portillo reservoirs (Supporting Information Figs. S2b, S5b, S6b). In San Clemente, La Bolera, Francisco Abellán, and Jándula reservoirs (sinks), we found a N_2O peak above the oxycline (Fig. 1a; Supporting Information Figs. S2–4a), and a decrease in N_2O to undersaturated values below the oxycline, reaching 37% in San Clemente reservoir, and 84% in La Bolera reservoir. In both systems, we detected high abundances of the *nosZ* gene that could explain the net consumption of N_2O during the last step of denitrification (i.e., the conversion of N_2O to N_2). In contrast, N_2O increased below the oxycline in reservoirs acting as sources, leading to massive accumulations of N_2O (Fig. 2a; Supporting Information Figs. S9a–S11a). In Iznájar, Béznar, and Cubillas reservoirs we detected high abundances of archaeal *amoA* gene and *nirS* gene at these sites, suggesting that the accumulation of N_2O may be produced by ammonia oxidizers or denitrifiers (Fig. 2a; Supporting Information Figs. S9a, S10a). Both processes have the highest yields of N_2O at low oxygen concentrations. We show the distribution of N_2O, dissolved oxygen (DO), and other chemical and biological variables in Supplementary Tables S3–S5 and in Supporting Information Fig. S12.

The wide range in N_2O concentration and % of saturation found in this study covers values reported in temperate and subtropical reservoirs (Deemer et al. 2011; Liang et al. 2019), and it is broader than the variability found in alpine and subtropical reservoirs (Diem et al. 2012; Musenze et al. 2014). The maximum N_2O concentration found in Iznájar reservoir was higher than the maximum values detected in surface and deep waters in other studies (Diem et al. 2012; Musenze et al. 2014; Beaulieu et al. 2015; Liang et al. 2019). Previous studies also detected peaks of N_2O at the oxic–anoxic interface in stratified lakes and reservoirs (Beaulieu et al. 2015), and large accumulations of N_2O below the oxycline of reservoirs (Deemer et al. 2011; Beaulieu et al. 2015). In a survey of 20 reservoirs, Beaulieu et al. (2015) also found that some reservoirs were supersaturated in N_2O, while others presented undersaturation values.

Biogeochemical control on N_2O concentration

N_2O concentration was a positive power function of the nitrogen content in different chemical forms in the water column (Supplementary Table S6). In particular, TN or nitrate concentration explained 43% of the variance in the N_2O concentration (Supporting Information Fig. S13). Besides, N_2O was also a negative power function of the oxygen availability

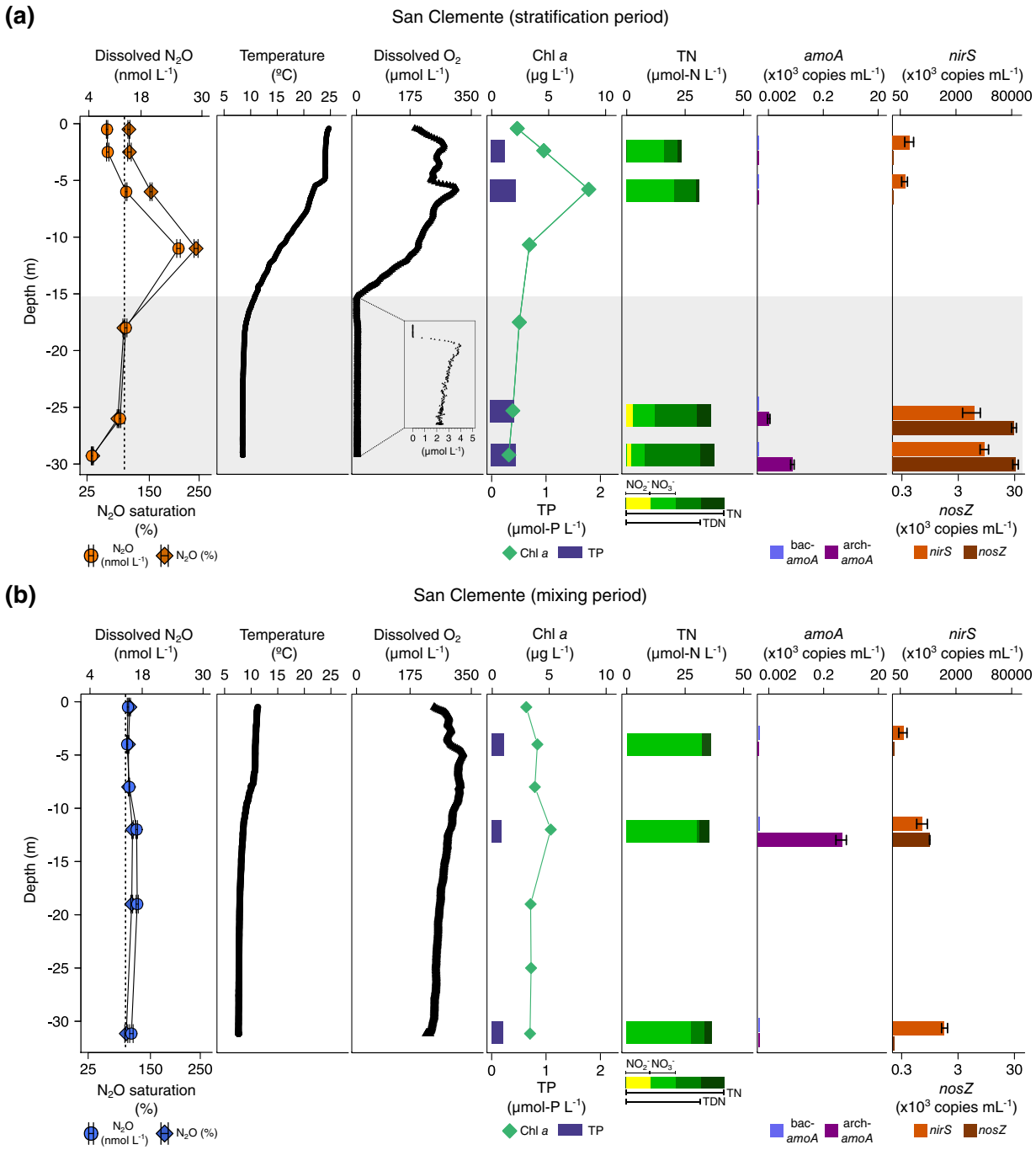

Fig. 1. Vertical profiles of physicochemical and biological variables in San Clemente reservoir. N_2O concentration (nmol L^{-1}, mean ± standard error, circles), N_2O saturation (%, mean ± standard error, diamonds), and atmospheric equilibrium concentration (discontinuous line); water temperature (°C); DO concentration (μmol L^{-1}); Chl *a* concentration (μg L^{-1}) and TP concentration (μmol-P L^{-1}); TN concentration (μmol-N L^{-1}); abundance of the *amoA* genes (bacterial *amoA* and archaeal *amoA*, × 10^3 copies mL^{-1}, mean ± standard deviation); and abundance of the *nirS* and *nosZ* genes (× 10^3 copies mL^{-1}, mean ± standard deviation) during the stratification period (**a**) and the mixing period (**b**). Note that the gene abundance axes are in logarithmic and different scale. The gray area represents the suboxic zone (DO < 10 μmol L^{-1}).

(Supporting Information Fig. S14). Combined in a GAM, nitrate and DO concentrations explained 64% of the variance in the N_2O concentration, and up to 81% of the variance when the interaction between both was included in the model (Fig. 3; Supplementary Table S7). The partial response of N_2O with respect to nitrate concentration shows a positive function (Fig. 3b), but negative with respect to DO concentration (Fig. 3c). Moreover, the model in Fig. 3a shows the interaction

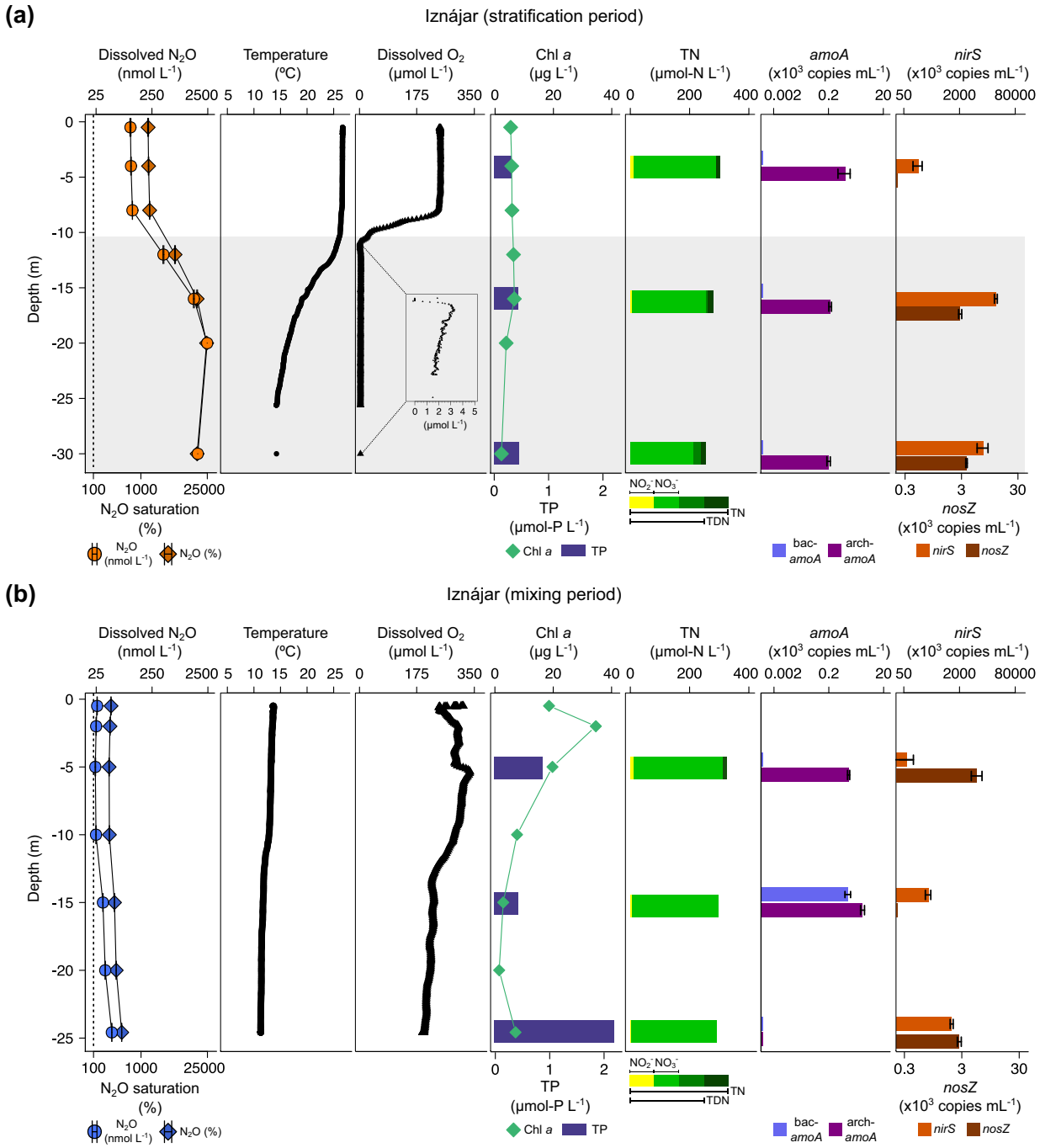

Fig. 2. Vertical profiles of physicochemical and biological variables in Iznájar reservoir. N_2O concentration (nmol L^{-1}, mean ± standard error, circles), N_2O saturation (%, mean ± standard error, diamonds), and atmospheric equilibrium concentration (discontinuous line); water temperature (°C); DO concentration (μmol L^{-1}); Chl *a* concentration (μg L^{-1}) and TP concentration (μmol-P L^{-1}); TN concentration (μmol-N L^{-1}); abundance of the *amoA* genes (bacterial *amoA* and archaeal *amoA*, × 10^3 copies mL^{-1}, mean ± standard deviation); and abundance of the *nirS* and *nosZ* genes (× 10^3 copies mL^{-1}, mean ± standard deviation) during the stratification period (**a**) and the mixing period (**b**). Note that the N_2O, and the gene abundance axes are in logarithmic and different scale. The gray area represents the suboxic zone (DO < 10 μmol L^{-1}).

between nitrate and DO concentrations. N_2O was consumed at low oxygen conditions when the nitrogen concentration was lower (i.e., sinks), but N_2O production increased at low oxygen conditions when the nitrogen concentration was higher (i.e., sources). The eight reservoirs that experienced suboxic conditions (DO < 10 μmol L^{-1}) in their hypolimnions during the summer stratification showed this trend: four of them were classified as sinks (i.e., Fig. 1a;

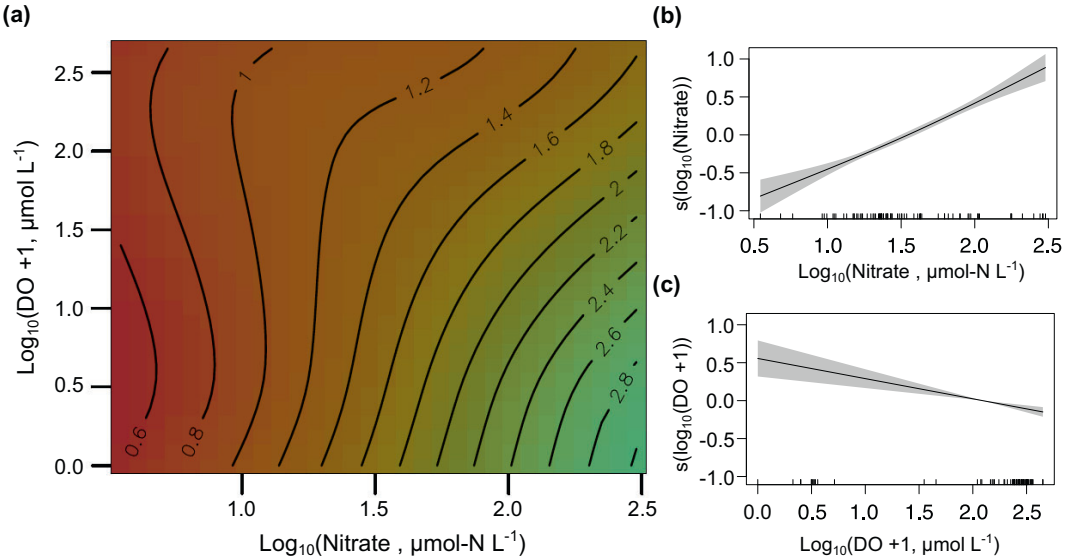

Fig. 3. GAM fitted to N_2O concentration ($\log_{10}$ N_2O, nmol L^{-1}), as function of nitrate ($\log_{10}$ NO_3^-, μmol-N L^{-1}), and DO concentration ($\log_{10}$ DO, μmol L^{-1}). (**a**) Contour plot showing the relationship between nitrate (x-axis) and DO (y-axis) with N_2O concentration (z-axis, contour lines). The model includes the interaction between nitrate and DO concentrations. Partial response plots showing the partial effects of (**b**) nitrate and (**c**) DO on N_2O concentration. Rugs on x-axis are the observed data points. The lines are the smoothing functions, and the shaded areas indicate the 95% confidence intervals. More details in Supplementary Table S6.

Supporting Information Figs. S2–4a) and four as sources (Fig. 2a; Supporting Information Figs. S9–S11a).

Nitrogen and oxygen availabilities control dissolved N_2O in the water column because they affect the microbial processes that determine the production and consumption of N_2O. These microbial processes will be further discussed in the next section. Previous studies demonstrated that N_2O is closely linked to N availability in freshwaters (e.g., Seitzinger et al. 2000; Beaulieu et al. 2011, 2015; Zhou et al. 2021). Beaulieu et al. (2015) found a positive relationship between mean epilimnion N_2O concentration and both NO_2^- and NO_3^- concentrations in reservoirs. In addition, they also found a net consumption of N_2O in the hypolimnions with low nitrogen content, but a net production in the hypolimnions with higher nitrogen content. Zhou et al. (2021) detected a positive relationship between the N availability (TN and nitrate) and N_2O fluxes in shallow lake sediments. In other aquatic environments, as the Chesapeake Bay, the production of N_2O was also controlled by nitrogen and oxygen availabilities (Ji et al. 2018).

Microbial groups affecting N_2O balance

Distribution and drivers of the microbial groups in the water column

The abundances of the bacterial and archaeal *amoA* (i.e., AOB and AOA), and the *nirS* and *nosZ* (i.e., denitrifying bacteria) genes are shown in Figs. 1, 2, Supporting Information Figs. S2–S11 and summarized in Supplementary Table S5. The archaeal *amoA* gene appeared in all the study reservoirs, but not in all the depths (i.e., 56 out of 77 samples), while the bacterial *amoA* gene appeared only in four samples. The median abundance of the archaeal *amoA* gene was 301 copies mL^{-1}, ranging from 0 to 1.9×10^4 copies mL^{-1}. The maximum abundances were in Los Bermejales, Negratín, and La Bolera reservoirs during the winter mixing (Supporting Information Figs. S8b, S5b, S2b). Archaeal *amoA* abundance did not show a significant relationship to the DO ($n = 77$, $p = 0.147$, Supporting Information Fig. S15a), or the nitrite concentration ($n = 77$, $p = 0.484$, Supporting Information Fig. S16). That may suggest that ammonium oxidation is coupled to nitrite oxidation. Previous studies in temperate lakes also found that AOA dominated over AOB (Small et al. 2013; Palacin-Lizarbe et al. 2019), while Pajares et al. (2017) found similar abundances of both groups in a tropical oligotrophic lake, with an abundance of the archaeal *amoA* gene similar to our study. Recent investigations pointed out that AOA may dominate over AOB in oligotrophic environments with a low ammonia supply (i.e., ocean; Martens-Habbena et al. 2009).

The *nirS* gene was ubiquitous, appearing in considerable abundances in the water column of all the reservoirs during both periods. We detected the maximum abundances of the *nirS* gene in Iznájar, Béznar, and Cubillas reservoirs during the stratification period together to high concentrations of N_2O (Fig. 2a; Supporting Information Figs. S9a, S10a). The median abundance of the *nirS* gene was 3.2×10^5 copies mL^{-1}, ranging from 0 to 1.1×10^8 copies mL^{-1}. We did not detect the *nirS* gene only in 8 samples out of 77, and we did not include these samples in the statistical tests since they were statistical

outliers ($G = 0.25$, $p < 0.001$). Besides, the *nirS* abundance was a negative power function to the DO concentration ($n = 69$, $p < 0.001$; Supporting Information Fig. S15b). The concentration of nitrate, which is the main substrate of denitrification, was not significantly related to the abundance of *nirS* gene, total prokaryotes, or the *nirS* : prokaryotes ratio (Supplementary Table S8; Supporting Information Fig. S17a–c). However, the *nirS* gene, and the *nirS* : prokaryotes ratio were negatively related to the nitrite concentration when the concentration was over detection level (Supporting Information Fig. S17e,f). We also found that TP concentration and cumulative Chl *a*, which is a proxy for the total phytoplanktonic biomass exported from the water column, were positive and significantly related to the abundance of the *nirS* gene, and, specifically, the *nirS* : prokaryotes ratio, but they were not related to the total abundance of prokaryotes (Fig. 4). Therefore, the effects of TP and cumulative Chl *a* are specific on the denitrifying bacteria (i.e., *nirS* gene). Together, DO and TP concentrations explained the abundance of denitrifiers in the water column of these reservoirs ($n = 69$, adj $R^2 = 0.68$, Supporting Information Fig. S18; Supplementary Table S9), showing the highest *nirS* abundances at low DO and high TP concentrations (Supporting Information Fig. S18a). On the other hand, we detected the *nosZ* gene in 37 out of 77 samples analyzed in oxic and suboxic conditions (Supporting Information Fig. S15c). The abundance of the *nosZ* gene ranged from 0 to 3.1×10^4 copies mL^{-1} (median = 0 copies mL^{-1}). The maximum abundances of the *nosZ* gene were in the hypolimnia of San Clemente and La Bolera reservoirs at suboxic conditions, where we also detected the lowest N_2O saturation values (i.e., 37%, and 86%; Fig. 1a; Supporting Information Fig. S2a).

The abundance of *nirS* gene is a biomarker for the denitrifying community, while the *nosZ* gene is a proxy for the bacteria that reduces N_2O to N_2, because this gene code the nitrous oxide reductase (Hallin et al. 2018). Our results indicate that denitrifying bacteria (i.e., *nirS* gene) are ubiquitous and very abundant in the water column of the study reservoirs. Besides, *nirS* abundance was 3 orders of magnitude higher (median = 3.2×10^5 copies mL^{-1}) than the abundance of the *amoA* gene (median = 301 copies mL^{-1}), and the *nosZ* gene (median = 0 copies mL^{-1}). *nirS* gene codes the nitrite reductase that reduce nitrite during denitrification, and that may explain its relationship with the nitrite concentration. In this study we targeted only *nirS*-type denitrifiers, however *nirK*-type denitrifiers may be also present in these systems.

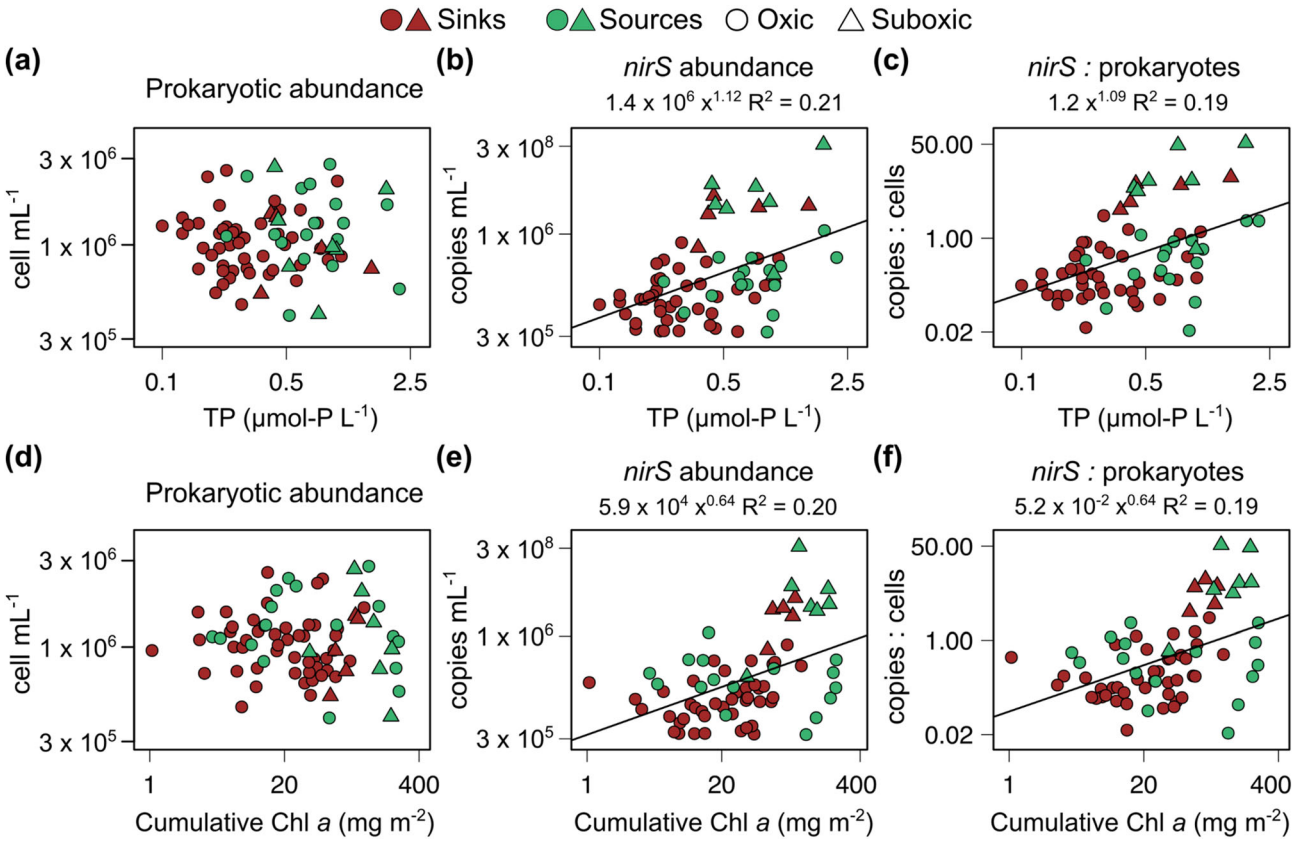

Fig. 4. Effect of the concentrations of (**a**–**c**) TP (μmol-P L^{-1}) and (**d**–**f**) cumulative Chl *a* (mg m^{-2}) on the abundance of (a, d) prokaryotes (cell mL^{-1}), (b, e) *nirS* gene (copies mL^{-1}), and the (c, f) *nirS* : prokaryotes ratio (*nirS* copies: prokaryotic cells). The brown dots stand for the reservoirs acting as sinks, while the green dots stand for the reservoirs acting as sources of N_2O. Note the log scales.

Few studies have analyzed the occurrence or distribution of the *nirS*, *nirK*, or *nosZ* genes in the water column of lakes or reservoirs (Junier et al. 2008; Kim et al. 2011; Pajares et al. 2017; Mao et al. 2017). Junier et al. (2008) and Kim et al. (2011) detected the *nirS* gene in the water column of lakes, with the higher diversity in the epilimnion, and different denitrifying communities in the water column and the sediments. The maximum abundance detected in our study was up to 3 orders of magnitude higher than the maximum detected by Pajares et al. (2017) in a tropical lake, who also described a similar abundance of the *nirK* gene, but the *nirS* abundance in our study was similar to the abundance detected by Mao et al. (2017). Mao et al. (2017) also detected the *nosZ* gene in the water column of lakes, with an abundance several orders of magnitude higher than the abundance detected in our work. In the study reservoirs, the occurrence of the gene *nosZ* was more limited than the occurrence of the *nirS* gene, and we only detected *nosZ* in about half the samples analyzed. This finding may reflect a real limitation in the distribution of the *nosZ* gene in the study reservoirs. However, this could also be due to a methodological limitation, as we may not have detected all *nosZ* gene variants by using primers that may only capture typical *nosZ* variants (Clade I). Nitrous oxide reductases reducing N_2O to N_2 are not always affiliated with denitrifying microorganisms. Recent findings showed that some organisms possess a Clade II (atypical) *nosZ* gene, and this atypical *nosZ* gene can even dominate marine microbiomes (Bertagnolli et al. 2020). *nirS* and *nosZ* genes were present in both oxic and suboxic conditions, but they showed a preference for low oxygen environments. *nirS* abundance was negatively related to the oxygen availability, and the *nosZ* abundance showed the highest abundances at low oxygen conditions. Therefore, DO concentration may affect, but not inhibit, denitrification. In this regard, previous studies stated that denitrification is a facultative anaerobic process, and its last step of N_2O reduction is strongly sensitive to even traces of oxygen (Dalsgaard et al. 2014). However, other studies detected the occurrence of denitrifying bacteria (i.e., *nirS nirK* and *nosZ* genes) in oxic and anoxic conditions in the lake water column (Junier et al. 2008; Kim et al. 2011; Mao et al. 2017; Pajares et al. 2017). Aerobic denitrifying bacteria occur in diverse environments, and the effect of DO may depend on the specific microorganism (Lloyd 1993).

In addition to DO, TP and cumulative Chl *a* concentrations in the water column had a specific positive effect on the denitrifier abundance (i.e., *nirS* and *nirS* : prokaryotes ratio). Pajares et al. (2017) also reported that phosphorus concentration was positively related to the abundance of denitrifiers in a tropical lake. Phosphorus is a rate-limiting nutrient in natural systems (Guignard et al. 2017), and may affect denitrifying bacteria replication or performance. In fact, the study of Arat et al. (2015) suggested that P availability affects denitrification gene expression. This study was based on the gene regulatory and metabolic network for the denitrification pathway in *Pseudomonas aeruginosa* PAO1 under different environmental conditions. They also confirmed experimentally that phosphate concentration increased N_2O production in *P. aeruginosa* cultures. Although this study was performed only with one bacterium, other denitrifying bacteria may have similar regulation systems, and that may explain the relationship between *nirS* gene abundance and TP concentration that we found in the study reservoirs. Much attention has been paid to the effect of nitrogen on the N_2O production or denitrification, but P results being a key nutrient, and it may have a more relevant role in denitrification that expected.

On the other hand, in this study the abundance of the *nirS* gene did not depend on DOC concentration (Supplementary Table S8), but it depended on the cumulative Chl *a* concentration. This relationship may suggest that denitrification is stimulated by fresh autochthonous organic matter, that can serve as labile carbon source, as they are heterotrophic organisms. This idea was also suggested by previous studies in freshwaters (McMillan et al. 2010; Chen et al. 2012). Denitrification rates in the ocean depend on the organic matter exported from the photic zone derived from primary production, and affected by the quality and quantity of organic matter (Kalvelage et al. 2013; Ward 2013*b*; Babbin et al. 2014). In addition, the high algal biomass of eutrophic reservoirs can result in hypoxia events that also stimulate denitrification. In the second place, this relationship may also suggest that denitrification and N_2O production in the water column is enhanced by sinking particles derived from the phytoplankton community (Zhou et al. 2019*b*).

Microbial control on N_2O concentration

We found that the N_2O concentration (nmol L^{-1}) depended on the *nirS* abundance (copies mL^{-1}) following a power function ($N_2O = 0.27\ nirS^{0.33}$, $n = 69$, adj $R^2 = 0.28$, $p < 0.001$; Fig. 5b). N_2O also depended on the *nirS* : prokaryotes ratio ($n = 69$, adj $R^2 = 0.22$, $p < 0.001$; Fig. 5e). However, N_2O was not significantly related to the abundances of *amoA* or *nosZ* separately (Fig. 5a,c). When we modeled the effect of the three genes on the N_2O using a GAM, we found that the abundance of *nosZ* also affected significantly the N_2O concentration, in combination with the *nirS* gene (Supplementary Table S10). Together, they explained up to 34% of the variance, and up to 40% when we used the gene: prokaryotes ratios (i.e., relative abundance) instead of the absolute gene abundances. We also studied the relationship between the *amoA* : *nirS* and the *nirS* : *nosZ* ratios with the N_2O, but the results were not significant (Supporting Information Fig. S19). Finally, we modeled the N_2O concentration in the water column as function of the concentration of the main substrate for denitrification (i.e., NO_3^-), and the relative abundance of denitrifiers, which are involved in the production (i.e., *nirS* : prokaryotes) and the consumption of N_2O (i. e., *nosZ* : prokaryotes ratios) (Fig. 6). N_2O concentration was a positive exponential function of the nitrate and the

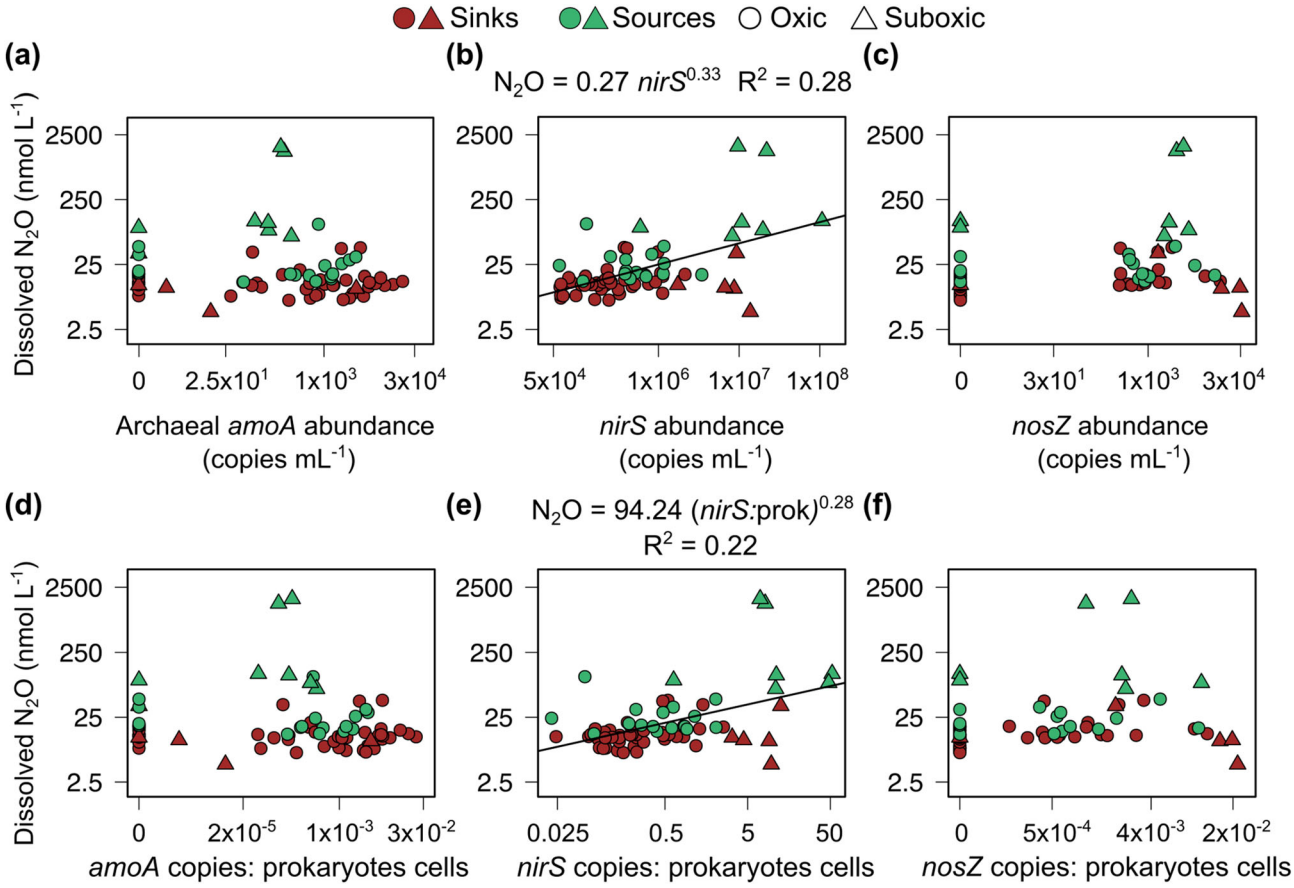

Fig. 5. Scatterplots of the dissolved N_2O concentration (nmol L^{-1}) and the abundance of the related groups: (**a**) archaeal *amoA* gene (copies mL^{-1}); (**b**) *nirS* gene ($n = 69$, $p < 0.001$); (**c**) *nosZ* gene; (**d**) archaeal *amoA* : prokaryotes ratio (*amoA* copies: prokaryotic cells); and (**e**) *nirS* : prokaryotes ratio (*nirS* copies: prokaryotic cells) ($n = 69$, $p < 0.001$); and (**f**) *nosZ* : prokaryotes ratio (*nosZ* copies: prokaryotic cells). Reservoirs acting as sinks are represented in brown, while reservoirs acting as sources of N_2O are represented in green. The dots stand for the oxic samples, and the triangles stand for the suboxic samples. Note the log scale in X and Y axes.

nirS : prokaryotes ratio, but a negative linear function of the *nosZ* : prokaryotes ratio. This model had an explained deviance of 68.3%, and adjusted R^2 of 0.66 ($n = 69$). We show the effect of the two-by-two explanatory variables on the N_2O in the contour plots (Fig. 6a,c,e), and the partial responses of each variable on the N_2O concentration in Fig. 6b,d,f. Further statistical details are provided in Supplementary Table S10.

Our results strongly suggest that denitrification may be the main microbial metabolism controlling the N_2O budget in the water column of the study reservoirs. In this work we modeled N_2O concentration as function of the nitrate and DO concentrations, with a negative interaction between both variables (Fig. 3), but also as function of nitrate and denitrifiers relative abundances (Fig. 6). Both models are connected. Nitrate and DO significantly affect denitrification. Nitrate is the substrate for denitrification, and its higher availability will determine a higher N_2O production, however the effect of DO differs depending on the N availability. Denitrifiers were present at oxic and suboxic conditions, but they were more abundant at low oxygen conditions, and they can both produce (i.e., *nirS* gene) and consume N_2O (i.e., *nosZ* gene). The undersaturated values for N_2O concentration were associated to low N and DO availabilities (Fig. 3a), where denitrifiers are abundant, but the low substrate availability may determine that they reduce N_2O to N_2 at a higher rate that they produce N_2O, leading to N_2O undersaturation. In contrast, the highest N_2O concentrations were located at high nitrate but low DO concentrations (Fig. 3a). At these conditions, denitrifiers have no substrate limitation and reach their higher N_2O yields. Previous studies have also suggested that denitrification may have a major role in N_2O production in different ecosystems. Zhou et al. (2019*a*) suggested that aerobic denitrification dominated the nitrogen losses in a reservoir. A previous survey in 17 shallow lakes also found a correlation between the abundance of denitrifiers (i.e., *nirS*/*nirK*) in lake sediments and N_2O fluxes (Zhou et al. 2021). Dai et al. (2022) found that archaeal *amoA* genes and transcripts were more dominant in the coastal and estuarine areas which had low nitrogen concentration, while

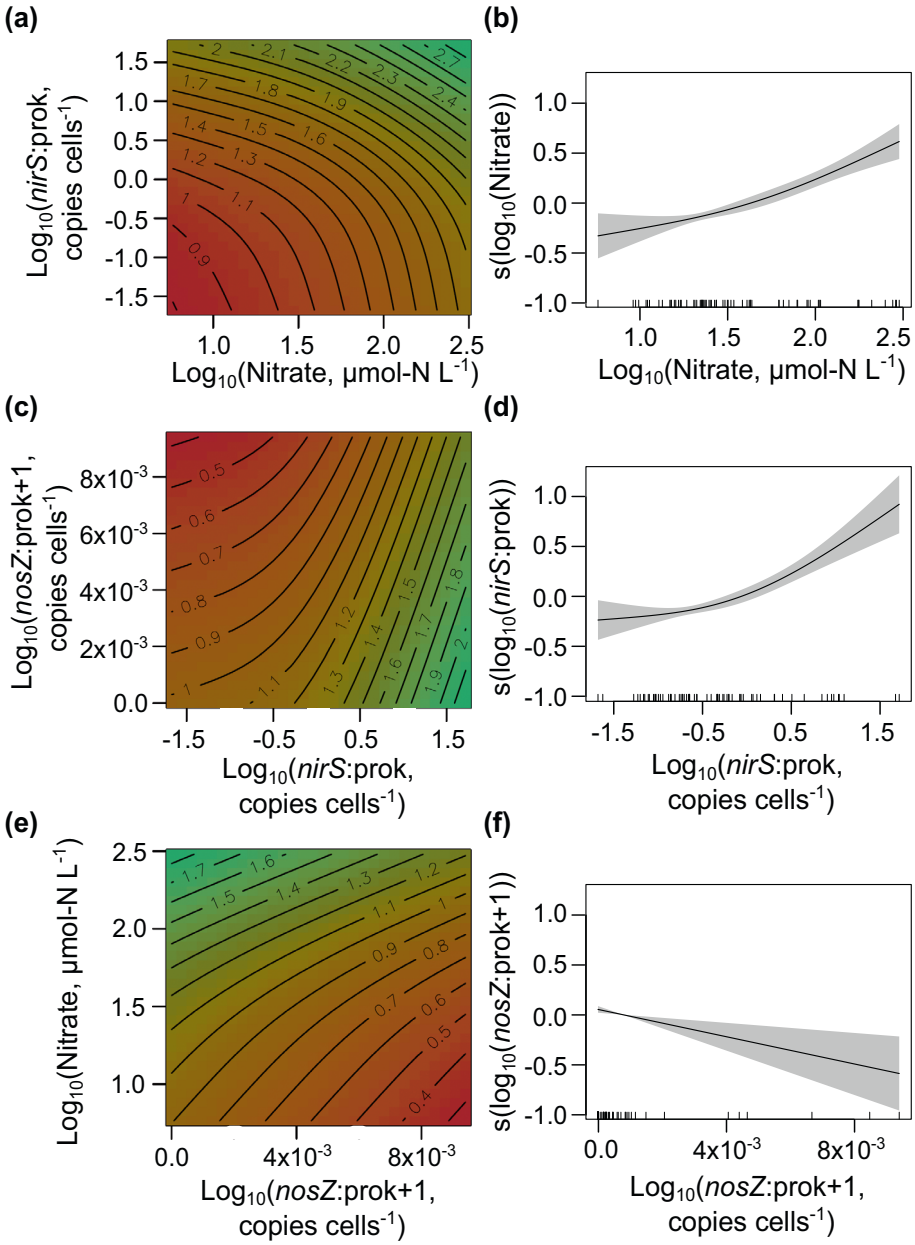

Fig. 6. GAM fitted to N_2O concentration (log_{10} N_2O, nmol L^{-1}), as function of nitrate (log_{10} NO_3^-, μmol-N L^{-1}), the *nirS* : prokaryotes ratio (log_{10} *nirS* : prokaryotes, copies $cells^{-1}$) and the *nosZ* : prokaryotes ratio (log_{10} *nosZ* : prokaryotes + 1, copies $cells^{-1}$). The effect of the explanatory variables on the N_2O concentration is shown in two-by-two contour plots (**a**, **c**, **e**) and on the individual partial response plots (**b**, **d**, **f**). Contour plot showing the relationship between (a) nitrate (x-axis) and *nirS* : prokaryotes (y-axis); (b) *nirS* : prokaryotes (x-axis) and *nosZ* : prokaryotes (y-axis); and (c) *nosZ* : prokaryotes (x-axis) and nitrate (y-axis) with the N_2O concentration (z-axis, contour lines). Individual partial response plots showing the partial effects of (b) nitrate, (d) *nirS* : prokaryotes, and (f) *nosZ* : prokaryotes in the model. Rugs on x-axis are the observed data points. The lines are the smoothing functions, and the shaded areas indicate the 95% confidence intervals. More details in Supplementary Table S10.

nirS genes and transcripts dominated in the areas of high nitrogen inputs. Based on the distribution patterns, the authors suggested that denitrification may control N_2O emissions. Li et al. (2016) found a positive correlation between *nirK* abundance and N_2O fluxes in composting piles, while a negative correlation between *nosZ* and N_2O fluxes.

On the other hand, this result does not mean that AOA are not contributing at all to N_2O budget. AOA may be producing N_2O, specially in some reservoirs or under specific conditions (i.e., suboxic waters), but their contribution is difficult to assess with this methodology. The analysis of functional genes as molecular markers for microbial processes is a widely

applied approach to understand biogeochemical processes in natural ecosystems. In particular, the abundances of *amoA*, *nirS*, or *nosZ* genes are frequently used to assess the contribution of these microbial groups to the N_2O budget (e.g., Löscher et al. 2012; Zhou et al. 2021). However, this methodology does not quantify the N_2O production or consumption rates. Therefore, the findings presented in this work should be confirmed using experimental measurements, as rates determination using ^{15}N-labeled substrates. Ammonia oxidation has been suggested as the primary process contributing to the N_2O production in oxic waters, but we did not find a significant relationship between the abundance of archaeal *amoA* gene and the dissolved N_2O concentration in the study reservoirs. The archaeal *amoA* gene has been extensively studied in the marine waters and sediments, where it is present in large numbers and contribute significantly to the N_2O production (e.g., Francis et al. 2005; Löscher et al. 2012; Trimmer et al. 2016). However, their role in N_2O production in freshwaters is less known.

An ecosystemic and global perspective

In essence, human activities in the watersheds of reservoirs determine their roles as sinks or sources of N_2O by increasing the inputs of nutrients, and then, modifying the activity and growth of the microbial community. Reservoirs classified in this study as N_2O sinks are located in watersheds with more than ~ 30% of forested areas, while the sources are located in agricultural and urban landscapes (León-Palmero et al. 2020*a*). Crops and urban areas exported nutrients to reservoirs by runoff, increasing the concentration of N and P in the water column, while forested areas had the oppositive effect (Supporting Information Fig. S20a–h) (León-Palmero et al. 2021). Besides, the effect of urban areas (%) showed a higher slope than in the crop areas, highlighting the higher impact of urban development in comparison to crop areas (Fig. 7). Land uses in the watershed were also significantly related to the N_2O concentrations and fluxes (Supporting Information Fig. S20i–p). Our findings are in agreement with previous works that show that nitrogen inputs into aquatic systems can boost the production and subsequent emission of N_2O (Seitzinger et al. 2000; Beaulieu et al. 2011, 2015; Baulch et al. 2011), although most of them focused on the agricultural effects (Baulch et al. 2011; Musenze et al. 2014; Beaulieu et al. 2015).

Therefore, a reservoir will change from acting as a sink to a source if it receives N and P inputs from agriculture and urban areas, which will affect denitrifying bacteria in different ways (Fig. 7). In this work we found that N inputs directly increase N_2O concentration, whereas P inputs increased the proliferation of denitrifiers. The increase in the Chl *a* concentration,

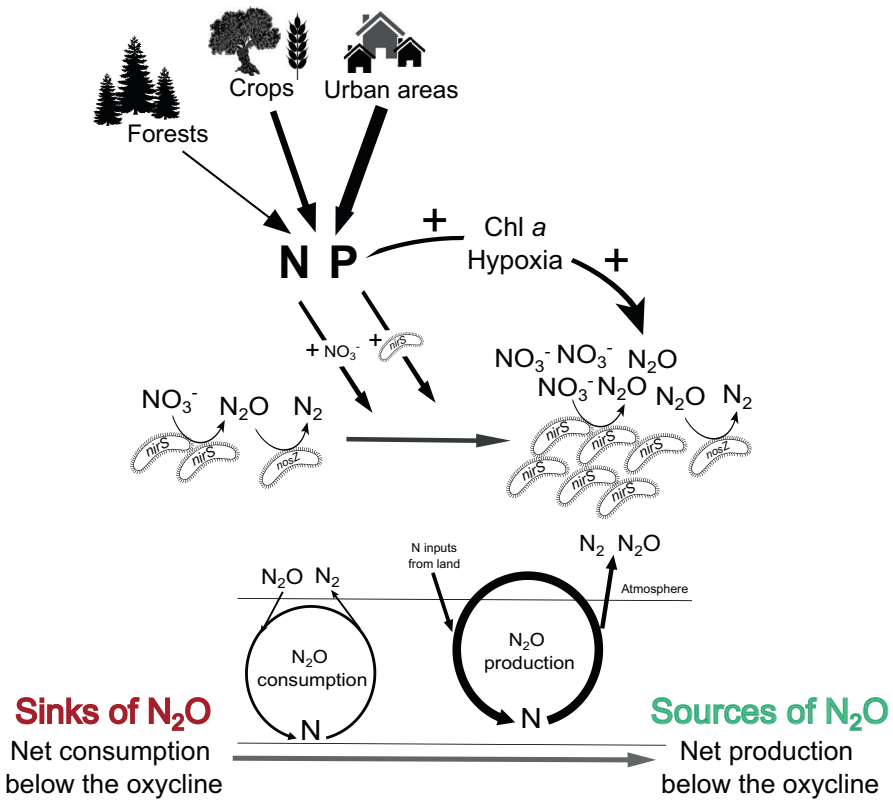

Fig. 7. Land uses in the watershed determine the N and P inputs that will modify the functioning of reservoirs, to change from a sink to a source of N_2O. The width of the arrows is proportional to the nutrient inputs from the watershed land uses. The circular model is inspired by Margalef (1983).

and the hypoxia events during the stratification period are also consequences of eutrophication that will also promote denitrification and N_2O production. DelSontro et al. (2018) also found that N_2O emission rates depended on Chl *a* in lakes and reservoirs. Nutrient-rich conditions and algal accumulation are important drivers of N_2O emissions, and these emissions may increase exponentially with the trophic state, as recently suggested in shallow lakes (Zhou et al. 2021). However, as explained previously, low oxygen conditions only increased the potential capacity of reducing N_2O to N_2 at low nitrogen concentrations. This behavior was more evident during the stratification than during the mixing period, because of the formation of the suboxic hypolimnion.

Margalef (1983) explained that freshwaters respond to the anthropogenic N and P inputs with negative feedbacks that displace a fraction of the materials to their corresponding boundaries. These boundaries are the sediments for the case of P, and the atmosphere for the case of N. In other words, an ecosystem that experiences N loading from human activities will accelerate denitrification to displace the excess N into the atmosphere, as N_2 and, especially, as the potent greenhouse gas N_2O. Therefore, from an ecosystemic point of view, denitrification acts as negative feedback process to release the excess of N inputs in the water column back toward the atmosphere, from where it was extracted first, artificially fixed by humans. Globally, half of the terrestrial denitrification occurs in freshwaters, with most of the nitrogen that is denitrified coming from the surrounding land (Seitzinger et al. 2006). In Fig. 7 we show a diagram summarizing the content of this work.

In this study we demonstrated that some reservoirs accumulate large concentrations of N_2O in their hypolimnions. The dissolved N_2O stored in deep waters will be emitted to the atmosphere via other pathways, such as the autumn overturn, or by degassing at the dam outflow or further downstream (i.e., indirect emissions). Unlike natural lakes, reservoirs have water intakes that connect the deep section of the water column and the downstream river, which provides water to the turbines to generate electricity. The turbulence and reduced pressure when the gas-rich water passes through the turbines and the pipes cause the degasification and direct emission of gases to the atmosphere at the dam outflow (i.e., degassing emissions) or the emission from the river surface below (i.e., downstream emission). Previous works have demonstrated that degassing and downstream emissions represent a significant fraction for N_2O emissions (Okuku et al. 2019). Reservoirs may have a relevant role in the N loss and N_2O emissions globally, especially from those ones located in agricultural and urban landscapes, while others in forested areas may uptake N_2O. Therefore, these results can be relevant for reservoir and watershed management, especially considering the plans for increasing the number of reservoirs worldwide (Zarfl et al. 2015). Future studies should consider how human activities can turn reservoirs being sinks to sources of N_2O, and how the dissolved N_2O produced or consumed in the water column can affect direct and indirect emissions from reservoirs.

References

Álvarez-Salgado, X. A., and A. E. J. Miller. 1998. Simultaneous determination of dissolved organic carbon and total dissolved nitrogen in seawater by high temperature catalytic oxidation: Conditions for precise shipboard measurements. Mar. Chem. **62**: 325–333. doi:10.1016/S0304-4203(98)00037-1

American Public Health Association (APHA). 1992. *In* A. E. Greenberg, L. S. Clesceri, and A. D. Eaton [eds.], Standard methods for the examination of water and wastewater, 18th ed. American Public Health Association.

Arat, S., G. S. Bullerjahn, and R. Laubenbacher. 2015. A network biology approach to denitrification in *Pseudomonas aeruginosa*. PloS One **10**: e0118235. doi:10.1371/journal.pone.0118235

Babbin, A. R., R. G. Keil, A. H. Devol, and B. B. Ward. 2014. Organic matter stoichiometry, flux, and oxygen control nitrogen loss in the ocean. Science **344**: 406–408. doi:10.1126/science.1248364

Baulch, H. M., S. L. Schiff, R. Maranger, and P. J. Dillon. 2011. Nitrogen enrichment and the emission of nitrous oxide from streams. Global Biogeochem. Cycles **25**: 15. doi:10.1029/2011GB004047

Beaulieu, J. J., C. T. Nietch, and J. L. Young. 2015. Controls on nitrous oxide production and consumption in reservoirs of the Ohio River basin. J. Geophys. Res. Biogeosci **120**: 1995–2010. doi:10.1002/2015JG002941

Beaulieu, J. J., and others. 2011. Nitrous oxide emission from denitrification in stream and river networks. Proc. Natl. Acad. Sci. **108**: 214–219. doi:10.1073/pnas.1011464108

Bertagnolli, A. D., K. T. Konstantinidis, and F. J. Stewart. 2020. Non-denitrifier nitrous oxide reductases dominate marine biomes. Environ. Microbiol. Rep. **12**: 681–692. doi:10.1111/1758-2229.12879

Bonin, P., M. Gilewicz, and J. C. Bertrand. 1989. Effects of oxygen on each step of denitrification on *Pseudomonas nautica*. Can. J. Microbiol. **35**: 1061–1064. doi:10.1139/m89-177

Caranto, J. D., and K. M. Lancaster. 2017. Nitric oxide is an obligate bacterial nitrification intermediate produced by hydroxylamine oxidoreductase. Proc. Natl. Acad. Sci. **114**: 8217–8222. doi:10.1073/pnas.1704504114

Chen, X., L. Yang, L. Xiao, A. Miao, and B. Xi. 2012. Nitrogen removal by denitrification during cyanobacterial bloom in Lake Taihu. J. Freshwater Ecol. **27**: 243–258. doi:10.1080/02705060.2011.644405

Dai, X., M. Chen, X. Wan, E. Tan, J. Zeng, N. Chen, S.-J. Kao, and Y. Zhang. 2022. Potential contributions of nitrifiers and denitrifiers to nitrous oxide sources and sinks in

China's estuarine and coastal areas. Biogeosciences **19**: 3757–3773. doi:10.5194/bg-19-3757-2022

Dalsgaard, T., F. J. Stewart, B. Thamdrup, L. D. Brabandere, N. P. Revsbech, O. Ulloa, D. E. Canfield, and E. F. DeLong. 2014. Oxygen at nanomolar levels reversibly suppresses process rates and gene expression in anammox and denitrification in the oxygen minimum zone off northern Chile. mBio **5**: e01966. doi:10.1128/mBio.01966-14

Deemer, B. R., J. A. Harrison, and E. W. Whitling. 2011. Microbial dinitrogen and nitrous oxide production in a small eutrophic reservoir: An in situ approach to quantifying hypolimnetic process rates. Limnol. Oceanogr. **56**: 1189–1199. doi:10.4319/lo.2011.56.4.1189

DelSontro, T., J. J. Beaulieu, and J. A. Downing. 2018. Greenhouse gas emissions from lakes and impoundments: Upscaling in the face of global change. Limnol. Oceanogr. Lett. **3**: 64–75. doi:10.1002/lol2.10073

Diem, T., S. Koch, S. Schwarzenbach, B. Wehrli, and C. J. Schubert. 2012. Greenhouse gas emissions (CO_2, CH_4, and N_2O) from several perialpine and alpine hydropower reservoirs by diffusion and loss in turbines. Aquat. Sci. **74**: 619–635. doi:10.1007/s00027-012-0256-5

Francis, C. A., K. J. Roberts, J. M. Beman, A. E. Santoro, and B. B. Oakley. 2005. Ubiquity and diversity of ammonia-oxidizing archaea in water columns and sediments of the ocean. Proc. Natl. Acad. Sci. **102**: 14683–14688. doi:10.1073/pnas.0506625102

Gasol, J. M., and P. A. del Giorgio. 2000. Using flow cytometry for counting natural planktonic bacteria and understanding the structure of planktonic bacterial communities. Sci. Mar. **64**: 197–224. doi:10.3989/scimar.2000.64n2197

Guignard, M. S., and others. 2017. Impacts of nitrogen and phosphorus: From genomes to natural ecosystems and agriculture. Front. Ecol. Evol. **5**: 70. doi:10.3389/fevo.2017.00070

Hallin, S., L. Philippot, F. E. Löffler, R. A. Sanford, and C. M. Jones. 2018. Genomics and ecology of novel N_2O-reducing microorganisms. Trends Microbiol. **26**: 43–55. doi:10.1016/j.tim.2017.07.003

Harrison, J. A., and others. 2009. The regional and global significance of nitrogen removal in lakes and reservoirs. Biogeochemistry **93**: 143–157. doi:10.1007/s10533-008-9272-x

Hink, L., P. Lycus, C. Gubry-Rangin, Å. Frostegård, G. W. Nicol, J. I. Prosser, and L. R. Bakken. 2017. Kinetics of NH3-oxidation, NO-turnover, N2O-production and electron flow during oxygen depletion in model bacterial and archaeal ammonia oxidisers. Environ. Microbiol. **19**: 4882–4896. doi:10.1111/1462-2920.13914

Inkscape Project. 2017. Inkscape: Open source scalable vector graphics editor. Free Software Foundation, Inc.

IPCC. 2013. Climate change 2013: The physical science basis. Contribution of working group I to the fifth assessment report of the intergovernmental panel on climate change. Cambridge Univ. Press.

Ji, Q., C. Frey, X. Sun, M. Jackson, Y.-S. Lee, A. Jayakumar, J. C. Cornwell, and B. B. Ward. 2018. Nitrogen and oxygen availabilities control water column nitrous oxide production during seasonal anoxia in the Chesapeake Bay. Biogeosciences **15**: 6127–6138.

Junier, P., O.-S. Kim, K.-P. Witzel, J. F. Imhoff, and O. Hadas. 2008. Habitat partitioning of denitrifying bacterial communities carrying *nirS* or *nirK* genes in the stratified water column of Lake Kinneret, Israel. Aquat. Microb. Ecol. **51**: 129–140. doi:10.3354/ame01186

Kalvelage, T., and others. 2013. Nitrogen cycling driven by organic matter export in the South Pacific oxygen minimum zone. Nat. Geosci. **6**: 228–234. doi:10.1038/ngeo1739

Kim, O.-S., J. F. Imhoff, K.-P. Witzel, and P. Junier. 2011. Distribution of denitrifying bacterial communities in the stratified water column and sediment–water interface in two freshwater lakes and the Baltic Sea. Aquat. Ecol. **45**: 99–112. doi:10.1007/s10452-010-9335-7

Könneke, M., A. E. Bernhard, J. R. de la Torre, C. B. Walker, J. B. Waterbury, and D. A. Stahl. 2005. Isolation of an autotrophic ammonia-oxidizing marine archaeon. Nature **437**: 543–546. doi:10.1038/nature03911

Kowalchuk, G. A., and J. R. Stephen. 2001. Ammonia-oxidizing bacteria: A model for molecular microbial ecology. Annu. Rev. Microbiol. **55**: 485–529. doi:10.1146/annurev.micro.55.1.485

Kozlowski, J. A., M. Stieglmeier, C. Schleper, M. G. Klotz, and L. Y. Stein. 2016. Pathways and key intermediates required for obligate aerobic ammonia-dependent chemolithotrophy in bacteria and Thaumarchaeota. ISME J. **10**: 1836–1845. doi:10.1038/ismej.2016.2

Lehner, B., and others. 2011. High-resolution mapping of the world's reservoirs and dams for sustainable river-flow management. Front. Ecol. Environ. **9**: 494–502. doi:10.1890/100125

León-Palmero, E., I. Reche, and R. Morales-Baquero. 2019. Light attenuation in southern Iberian Peninsula reservoirs. Ing. Agua **23**: 65–75. doi:10.4995/ia.2019.10655

León-Palmero, E., R. Morales-Baquero, and I. Reche. 2020*a*. Greenhouse gas fluxes from reservoirs determined by watershed lithology, morphometry, and anthropogenic pressure. Environ. Res. Lett. **15**: 044012. doi:10.1088/1748-9326/ab7467

León-Palmero, E., A. Contreras-Ruiz, A. Sierra, R. Morales-Baquero, and I. Reche. 2020*b*. Dissolved CH_4 coupled to photosynthetic picoeukaryotes in oxic waters and to cumulative chlorophyll *a* in anoxic waters of reservoirs. Biogeosciences **17**: 3223–3245. doi:10.5194/bg-17-3223-2020

León-Palmero, E., R. Morales-Baquero, and I. Reche. 2020*c*. Location, morphometry, lithology and land-use in the watersheds of reservoirs in southern Spain. PANGAEA. doi:10.1594/PANGAEA.912540

León-Palmero, E., R. Morales-Baquero, and I. Reche. 2020*d*. Dissolved concentrations of CH_4, nutrients, and biological

parameters in the water column of twelve Mediterranean reservoirs in southern Spain. PANGAEA. doi:10.1594/PANGAEA.912535

León-Palmero, E., I. Reche, and R. Morales-Baquero. 2021. Land-use on the watershed determines the quality of water in South-Eastern Iberian Peninsula reservoirs. Ing. Agua **25**: 205–213. doi:10.4995/ia.2021.15690

Li, S., L. Song, Y. Jin, S. Liu, Q. Shen, and J. Zou. 2016. Linking N_2O emission from biochar-amended composting process to the abundance of denitrify (nirK and nosZ) bacteria community. AMB Express **6**: 37. doi:10.1186/s13568-016-0208-x

Liang, X., T. Xing, J. Li, B. Wang, F. Wang, C. He, L. Hou, and S. Li. 2019. Control of the hydraulic load on nitrous oxide emissions from cascade reservoirs. Environ. Sci. Technol. **53**: 11745–11754. doi:10.1021/acs.est.9b03438

Lloyd, D. 1993. Aerobic denitrification in soils and sediments: From fallacies to factx. Trends Ecol. Evol. **8**: 352–356. doi:10.1016/0169-5347(93)90218-E

Löscher, C. R., A. Kock, M. Könneke, J. LaRoche, H. W. Bange, and R. A. Schmitz. 2012. Production of oceanic nitrous oxide by ammonia-oxidizing archaea. Biogeosciences **9**: 2419–2429. doi:10.5194/bg-9-2419-2012

Mao, G., L. Chen, Y. Yang, Z. Wu, T. Tong, Y. Liu, and S. Xie. 2017. Vertical profiles of water and sediment denitrifiers in two plateau freshwater lakes. Appl. Microbiol. Biotechnol. **101**: 3361–3370. doi:10.1007/s00253-016-8022-6

Margalef, R. 1983. Capítulo 18: Ecosistemas forzados. Omega, p. 1010.

Martens-Habbena, W., P. M. Berube, H. Urakawa, J. R. de la Torre, and D. A. Stahl. 2009. Ammonia oxidation kinetics determine niche separation of nitrifying archaea and bacteria. Nature **461**: 976–979. doi:10.1038/nature08465

McCrackin, M. L., and J. J. Elser. 2011. Greenhouse gas dynamics in lakes receiving atmospheric nitrogen deposition. Global Biogeochem. Cycles **25**: GB4005. doi:10.1029/2010GB003897

McMillan, S. K., M. F. Piehler, S. P. Thompson, and H. W. Paerl. 2010. Denitrification of nitrogen released from senescing algal biomass in coastal agricultural headwater streams. J. Environ. Qual. **39**: 274–281. doi:10.2134/jeq2008.0438

Musenze, R. S., A. Grinham, U. Werner, D. Gale, K. Sturm, J. Udy, and Z. Yuan. 2014. Assessing the spatial and temporal variability of diffusive methane and nitrous oxide emissions from subtropical freshwater reservoirs. Environ. Sci. Technol. **48**: 14499–14507. doi:10.1021/es505324h

Okuku, E. O., S. Bouillon, M. Tole, and A. V. Borges. 2019. Diffusive emissions of methane and nitrous oxide from a cascade of tropical hydropower reservoirs in Kenya. Lakes Reserv. Sci. Policy Manag. Sustain. Use **24**: 127–135. doi:10.1111/lre.12264

Pajares, S., M. Merino-Ibarra, M. Macek, and J. Alcocer. 2017. Vertical and seasonal distribution of picoplankton and functional nitrogen genes in a high-altitude warm-monomictic tropical lake. Freshw. Biol. **62**: 1180–1193. doi:10.1111/fwb.12935

Palacin-Lizarbe, C., L. Camarero, S. Hallin, C. M. Jones, J. Cáliz, E. O. Casamayor, and J. Catalan. 2019. The DNRA-denitrification dichotomy differentiates nitrogen transformation pathways in mountain lake benthic habitats. Front. Microbiol. **10**: 1229. doi:10.3389/fmicb.2019.01229

Piña-Ochoa, E., and M. Álvarez-Cobelas. 2006. Denitrification in aquatic environments: A cross-system analysis. Biogeochemistry **81**: 111–130. doi:10.1007/s10533-006-9033-7

R Core Team. 2019. R: A language and environment for statistical computing. R Foundation for Statistical Computing.

Ravishankara, A. R., J. S. Daniel, and R. W. Portmann. 2009. Nitrous oxide (N_2O): The dominant ozone-depleting substance emitted in the 21st century. Science **326**: 123–125. doi:10.1126/science.1176985

Seitzinger, S. P., C. Kroeze, and R. V. Styles. 2000. Global distribution of N_2O emissions from aquatic systems: Natural emissions and anthropogenic effects. Chemosphere-Glob. Change Sci. **2**: 267–279. doi:10.1016/S1465-9972(00)00015-5

Seitzinger, S., J. A. Harrison, J. K. Böhlke, A. F. Bouwman, R. Lowrance, B. Peterson, C. Tobias, and G. V. Drecht. 2006. Denitrification across landscapes and waterscapes: A synthesis. Ecol. Appl. **16**: 2064–2090.

Sierra, A., D. Jiménez-López, T. Ortega, R. Ponce, M. J. Bellanco, R. Sánchez-Leal, A. Gómez-Parra, and J. Forja. 2017. Distribution of N_2O in the eastern shelf of the Gulf of Cadiz (SW Iberian Peninsula). Sci. Total Environ. **593–594**: 796–808. doi:10.1016/j.scitotenv.2017.03.189

Small, G. E., G. S. Bullerjahn, R. W. Sterner, B. F. N. Beall, S. Brovold, J. C. Finlay, R. M. L. McKay, and M. Mukherjee. 2013. Rates and controls of nitrification in a large oligotrophic lake. Limnol. Oceanogr. **58**: 276–286. doi:10.4319/lo.2013.58.1.0276

Soued, C., P. A. del Giorgio, and R. Maranger. 2015. Nitrous oxide sinks and emissions in boreal aquatic networks in Québec. Nat. Geosci. **9**: 116–120. doi:10.1038/ngeo2611

Stein, L. Y. 2019. Insights into the physiology of ammonia-oxidizing microorganisms. Curr. Opin. Chem. Biol. **49**: 9–15. doi:10.1016/j.cbpa.2018.09.003

Trimmer, M., P.-M. Chronopoulou, S. T. Maanoja, R. C. Upstill-Goddard, V. Kitidis, and K. J. Purdy. 2016. Nitrous oxide as a function of oxygen and archaeal gene abundance in the North Pacific. Nat. Commun. **7**: 1–10. doi:10.1038/ncomms13451

Ward, B. B. 2013*a*. Nitrification, p. 351–358. *In* B. Fath [ed.], Encyclopedia of ecology, 2nd ed. Elsevier.

Ward, B. B. 2013*b*. How nitrogen is lost. Science **341**: 352–353. doi:10.1126/science.1240314

Weiss, R. F., and B. A. Price. 1980. Nitrous oxide solubility in water and seawater. Mar. Chem. **8**: 347–359. doi:10.1016/0304-4203(80)90024-9

Wetzel, R. G. 2001. Limnology: Lake and river ecosystems. Eos Trans Am Geophys Union **21**: 1–9.

Wood, S. N. 2006. Generalized additive models: An introduction with R. Chapman and Hall/CRC.

Wrage, N., G. L. Velthof, M. L. van Beusichem, and O. Oenema. 2001. Role of nitrifier denitrification in the production of nitrous oxide. Soil Biol. Biochem. **33**: 1723–1732. doi:10.1016/S0038-0717(01)00096-7

Zarfl, C., A. E. Lumsdon, J. Berlekamp, L. Tydecks, and K. Tockner. 2015. A global boom in hydropower dam construction. Aquat. Sci. **77**: 161–170. doi:10.1007/s00027-014-0377-0

Zhou, S., Y. Zhang, T. Huang, Y. Liu, K. Fang, and C. Zhang. 2019*a*. Microbial aerobic denitrification dominates nitrogen losses from reservoir ecosystem in the spring of Zhoucun reservoir. Sci. Total Environ. **651**: 998–1010. doi:10.1016/j.scitotenv.2018.09.160

Zhou, Y., X. Xu, R. Han, L. Li, Y. Feng, S. Yeerken, K. Song, and Q. Wang. 2019*b*. Suspended particles potentially enhance nitrous oxide (N_2O) emissions in the oxic estuarine waters of eutrophic lakes: Field and experimental evidence. Environ. Pollut. **252**: 1225–1234. doi:10.1016/j.envpol.2019.06.076

Zhou, Y., and others. 2021. Nonlinear pattern and algal dual-impact in N_2O emission with increasing trophic levels in shallow lakes. Water Res. **203**: 117489. doi:10.1016/j.watres.2021.117489

Acknowledgments

We especially thank Eulogio Corral and Alba Contreras-Ruiz for helping in the field, and laboratory work, respectively. We also thank Ana Sierra, Jesús Forja and Teodora Ortega for helping with gas chromatography analysis at the University of Cádiz. We thank Amal Jayakumar from Ward Lab at Princeton University for the training in qPCR. We thank the Confederación Hidrográfica del Guadalquivir and the Agencia Andaluza del Medio Ambiente y Agua (AMAYA) for facilitating the reservoir sampling. This research was supported by the Ministerio de Economía y Competitividad (HERA project, grant no. CGL2014-52362-R), and the Ministerio de Ciencia, Innovación y Universidades (CRONOS project, RTI2018-098849-B-I00) of Spain to IR and RM-B. Elizabeth León-Palmero was supported by a PhD fellowship from the Ministerio de Educación, Cultura y Deporte of Spain (grant nos. FPU014/02917), and a postdoctoral contract from CRONOS project, and later from Danmarks Frie Forskningsfond (DFF, 1026-00428B) at SDU. This manuscript was improved through feedback from an anonymous reviewer, and Dr. Van Meter. Universidad de Granada/CBUA funded the open access of this article.

Conflict of Interest

The authors declare no competing financial interest.

Data Availability Statement

Data supporting the findings of this study are available within article, and in the Supplementary Information, and raw data are available on request from the authors.

Submitted 06 May 2022
Revised 01 February 2023
Accepted 18 May 2023

Associate editor: Kimberly Van Meter